IOP PUBLISHING PHYSICS IN MEDICINE AND BIOLOGY

Phys. Med. Biol. **53** (2008) 3681–3695 doi:10.1088/0031-9155/53/13/019

Analysis of RF exposure in the head tissues of children and adults

J Wiart[1], **A Hadjem**[1], **M F Wong**[1] **and I Bloch**[2]

[1] France Telecom R&D, Issy les Moulineaux, France
[2] Ecole Nationale Supérieure des Télécommunications, TELECOM ParisTech, Paris, France

E-mail: joe.wiart@orange-ftgroup.com

Received 9 November 2007, in final form 5 May 2008
Published 18 June 2008
Online at stacks.iop.org/PMB/53/3681

Abstract

This paper analyzes the radio frequencies (RF) exposure in the head tissues of children using a cellular handset or RF sources (a dipole and a generic handset) at 900, 1800, 2100 and 2400 MHz. Based on magnetic resonance imaging, child head models have been developed. The maximum specific absorption rate (SAR) over 10 g in the head has been analyzed in seven child and six adult heterogeneous head models. The influence of the variability in the same age class is carried out using models based on a morphing technique. The SAR over 1 g in specific tissues has also been assessed in the different types of child and adult head models. Comparisons are performed but nevertheless need to be confirmed since they have been derived from data sets of limited size. The simulations that have been performed show that the differences between the maximum SAR over 10 g estimated in the head models of the adults and the ones of the children are small compared to the standard deviations. But they indicate that the maximum SAR in 1 g of peripheral brain tissues of the child models aged between 5 and 8 years is about two times higher than in adult models. This difference is not observed for the child models of children above 8 years old: the maximum SAR in 1 g of peripheral brain tissues is about the same as the one in adult models. Such differences can be explained by the lower thicknesses of pinna, skin and skull of the younger child models.

(Some figures in this article are in colour only in the electronic version)

1. Introduction

Wireless systems are increasingly used; in particular, the number of children using a cellular handset or a cordless phone at home has increased in the past few years. Limits to protect general public, including children, from overexposure to electromagnetic fields are recommended by international bodies such as the International Commission on Non Ionizing

 © 2008 Institute of Physics and Engineering in Medicine

Radiation Protection (ICNIRP 1998) or the International Committee on Electromagnetic Safety (ICES) (IEEE 2005). Since questions were still open, the World Heath Organization (WHO) has set up in 1996 the EMF Project (EMF project 1996) to promote and coordinate the worldwide research. Expert groups have been set up and reports have been issued (SSI 2006, MTHR 2007). *In vivo* as well as epidemiological studies (Dasembrock 2005, Tillmann *et al* 2007, Collatz-Christensen *et al* 2005) have been performed, nevertheless there is still a public concern and in particular about the exposure of children to radio frequencies (RF). Recent reviews and studies (Martens 2005, Kheifets *et al* 2005, Juutilainen 2005) have discussed the sensitivity of children to electromagnetic fields (EMF). In 2004, WHO organized in Istanbul (Repacholi *et al* 2005) a workshop on children exposure that has emphasized the importance of the dosimetry (Christ and Kuster 2005).

The exposure assessment in adult heads and in particular the specific absorption rate (SAR) in tissues has been analyzed mainly using the Visible Human (VH) heterogeneous head model (Visible Human Project). VH is one of the first heads that have been built and has been intensively used since it has a 1 mm resolution but other adult head models have also been developed and recently used (Nagaoka *et al* 2004). The morphologies (size, weight, shape, etc) of these models as well as their spatial resolutions (voxel size) are different and influence the power absorbed by the tissues.

Dealing with children exposure, numerical studies (Schoenborn *et al* 1998, Gandhi *et al* 1996, Wang and Fujiwara 2003, Hadjem *et al* 2005, Wiart *et al* 2005, Beard *et al* 2006, Kainz *et al* 2005, De Salles *et al* 2006, Keshvari *et al* 2006) have also been conducted to analyze the electromagnetic absorption of RF and SAR in children tissues. Depending on the study, the RF exposure in child models is either higher than in adult models (Gandhi *et al* 1996, De Salles *et al* 2006) or similar (Schoenborn *et al* 1998, Wang and Fujiwara 2003, Hadjem *et al* 2005, Wiart *et al* 2005, Beard *et al* 2006, Kainz *et al* 2005). Various models have been used; the first models were based on a uniform downsizing of adult heads. However, a child head is not a reduced adult head. For instance the brain of a child grows quickly up to the age of three and reaches adult size between 6 and 14 years of age but at the age of 5 the brain weight is about 90% of the adult brain weight (Huttenlocher 1979). To overcome these limitations and since only few magnetic resonance imaging (MRI)-based models were available, other studies were performed (Wang and Fujiwara 2003, Hadjem *et al* 2005, Beard *et al* 2006) with child head models based on adult head models downscaled through a nonuniform downsizing taking into account the variation of the head shape with age. The limits of these studies are linked to the internal anatomy: tissues such as skin or skull have different growth rates and any downsizing can lead to a wrong internal tissues distribution. In spite of their limitations these studies showed that the anatomy, the model of the handset and the position of the handset relative to the head have a large influence on the SAR induced in the tissues.

Any comparison between adults and children faces the large variability of the head shape which evolves with age but also differs from one individual to another. For this reason, it is difficult to generalize any comparison between the SAR induced in two given heads (adults or children). Depending on the model resolution (and its influence on the internal tissues description), on the cheek shape and on the pinna thickness of the model, the SAR estimated in a model can be different. This explains some of the differences observed in different studies (Christ and Kuster 2005, Wiart *et al* 2005, Lee *et al* 2007, Mochizuki *et al* 2007).

The objective of the present study is to overcome the limitations of the previous studies by using several anatomically correct child and adult head models. Seven child head models have been used. Six child head models (from 5 years old to 15 years old) have been built for this study using MRI. The seventh child head model is a model of a 7 year old child which is commercially available (European Child Head Model EC 7 Speag&Partner), The

SAR induced in the tissues of these models has been compared to the SAR induced in six adult head models available worldwide. In this study, the hand is not taken into account since previous studies showed that the hand does not affect the SAR distribution (Watanabe *et al* 1996).

The dielectric properties of tissues evolve with age and may influence the absorption of tissues. Because of the higher conductivity reported for young rats (Peyman *et al* 2002), the use of dielectric properties (Gabriel 1996) commonly assigned to adult tissues for the child tissues has raised concerns. Based on Lichtenecker's law (Lichtenecker 1926), a study has been performed (Wang *et al* 2006) to analyze the influence of dielectric properties on SAR. This study has reported that the dielectric properties for the child head models do not affect significantly the 1 or 10 g averaged spatial peak SAR. Considering such results and taking into account that in this study the head models are derived from children older than 5 years of age, we focus our analysis on the morphology change and use for the child models the same dielectric properties as the ones used for the adult models.

2. Head models

2.1. Child head models based on MRI

For this study, several MRI datasets of children at different ages from three different French hospitals were available. The acquisitions are T1 weighted spoiled gradient recalled (SPGR) images and have a spatial resolution of about $1 \times 1 \times 1.2$ mm^3. They cover the whole head, thus allowing 3D segmentations of the main tissues from which realistic head models are derived.

In this section, we summarize the segmentation process, which is an original part of this study (Burguet *et al* 2004). The few existing child head models rely on a manual segmentation on 2D slices, resulting in a poor 3D spatial consistency, which is a major drawback for deriving relevant models. In contrast, the proposed method exploits the 3D nature of the data and performs all segmentation steps directly in the 3D space. By that way a good surface regularity of the tissues and structures is obtained.

These steps rely on the analysis of gray levels of each tissue or structure and on their geometry and shape, through mathematical morphology tools (Serra 1982). The segmentation method for skin, skull, brain, cerebro-spinal fluid (CSF), fat and muscle is an extension of the method described in Dokladal *et al* (2003) for adult heads. In particular, the segmentation parameters are automatically adapted based on existing knowledge on the variation of tissue thickness in different parts of the head during the child growth (Drossos *et al* 2000). The precise separation between skull and air is more difficult. We propose an approach based on the registration of a CT skull acquisition, which provides an initial segmentation of the skull in MRI, followed by a refinement of the segmentation using gradient vector flow (GVF) deformable models (Xu and Prince 1998). In all the cases more than ten tissues have been segmented and in particular skin, skull, fat, CSF, gray matter and white matter. Figure 1 illustrates a few results on a 5 year old child's head. Three orthogonal slices of the 3D segmented volume are displayed (each color corresponds to a type of tissue).

The final segmentation results are then transformed into a mesh suitable for further analysis. Six child head models (figure 2) at different ages (5, 6, 8, 9, 12 and 15 years old) have been built using this approach. As seen in figure 2, the children can be sleepy during the MRI acquisition. To avoid any respiratory problem, the children below 5 years old have a tube in the mouth that induces some deviation from standard anatomy but does not influence the area close to the ear, which is the most important for our concern. As explained in the

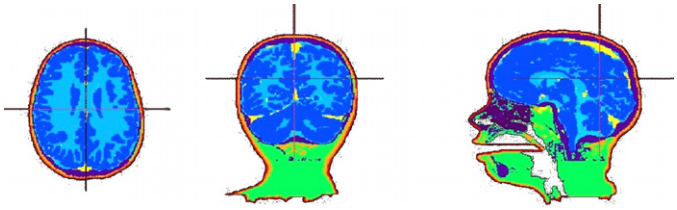

Figure 1. Segmented model of a 5 year old child (three orthogonal slices).

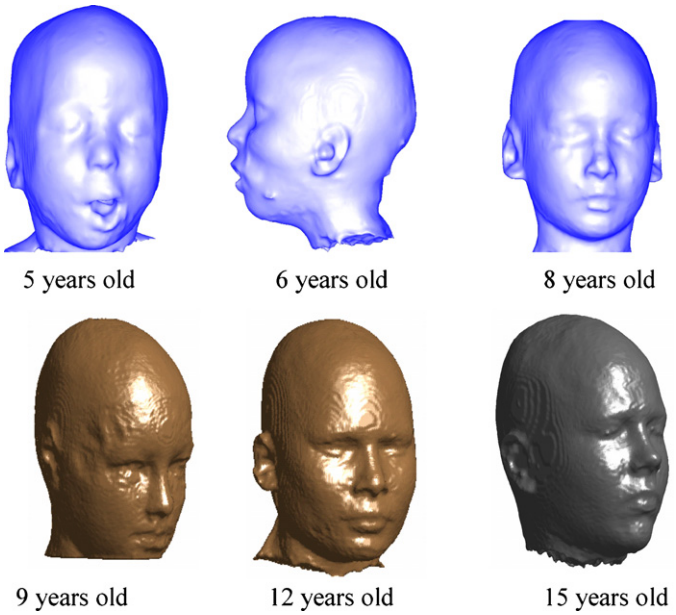

Figure 2. Child head models at different ages (5, 6, 8, 9, 12 and 15 years old) developed for this study.

introduction, a 7 year old child model based on MRI and developed in Switzerland has also been included in the study.

Since the SAR in tissues depends on the local anatomy, it is of interest to analyze the characteristics of the child head models used in this study with respect to those described in the literature (Farkas 1994, Huttenlocher 1979, Reißenweber *et al* 2005). Figure 3 shows the weight of muscle, skin and skull in the different models. The brain weights of the models are close to the mean value provided in the literature (Huttenlocher 1979). Nevertheless the models of 6 and 15 years old have brain weights 20% below the mean value. The weight of the skin of the 12 year old child model is the highest. This could be due to the large variability in children morphology but may also be due to the segmentation.

By comparing the shape of the 12 years old model to the literature (Farkas 1994) we have noticed that its height (21 cm) is smaller than the mean (minus one standard deviation) in contrast with the width (19.5 cm) which is larger than the mean (plus one standard deviation). Moreover the skin thickness also depends on age: for children around 12 years old, the skin thickness is about 1.56 mm $\pm$ 0.36 mm (Seidenari *et al* 2000).

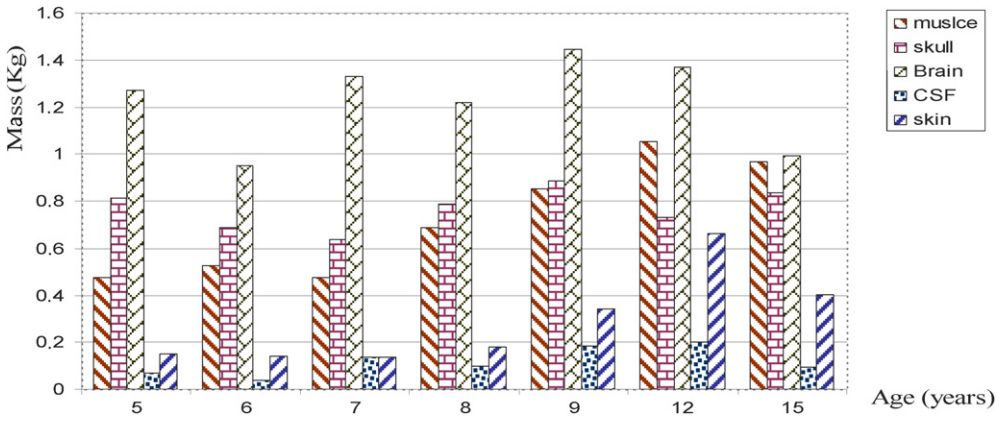

Figure 3. Weight of tissues in the child models versus age.

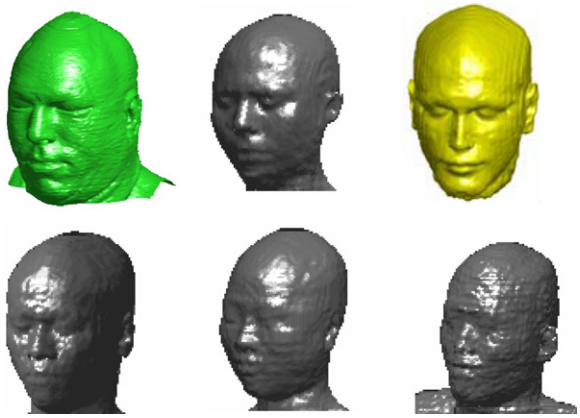

Figure 4. Adult Head models used in the study (from left to right and top to bottom: VH, Norman, FTRD, Japanese male, Japanese female and Korean male).

2.2. Adult head models

Worldwide several adult head models have been developed during the past few years. In this study we used six different models (figure 4): the VH head model from Visible Human Project segmented at Brooks Air Force, the NORMAN male model developed at HPA – NRPB (Dimbylow 1997), the model developed at France Telecom R&D named FTRD, the male and female models developed in Japan (Nagaoka *et al* 2004) and the last one is the male model developed in Korea (Kim *et al* 2006).

The resolutions of these models are different. The VH and Korean head models have a 1 mm resolution, the Japanese models (male and female) have a 2 mm resolution, FTRD has a 3 mm $\times$ 1 mm $\times$ 1 mm resolution and Norman has a 3 mm resolution. In this study we decided not to incorporate the model developed at Yale University (Zubal *et al* 1994) since its resolution of 3.6 mm does not allow an accurate description of fine internal structures and overestimates the skin proportion. Large differences between head phantoms exist (e.g. in terms of mass ratio skin represents 5% of the head mass of the Japanese male versus 10% in

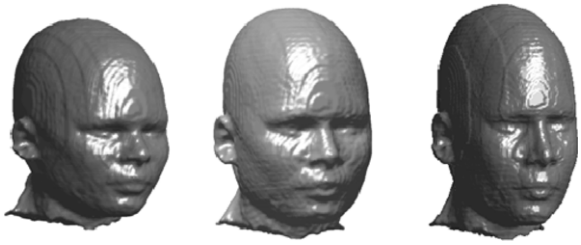

Figure 5. Head models derived from a 12 years old MRI-based child head model (from left to right: mean − 2 standard deviations, mean, mean + 2 standard deviations).

the VH model and 17% in the Korean model). As discussed for children, such differences can be explained by the large variability of the human morphology and the segmentation process and also by the voxel size.

2.3. 12 year old child head models based on MRI and morphing

In a same age class, child heads are different; however, MRI-based models remain limited in number. To investigate the influence of parameters such as pinna thickness and head shapes that could influence the SAR (Christ and Kuster 2005), we built models using a morphing technique (Wang and Fujiwara 2003, Hadjem *et al* 2005). This approach is based on a piecewise modification of a model by respecting the main anatomical parameters (Farkas 1994). Using data on the thickness of the pinna we built three new 12 years old models having pinna sizes (length, width, thickness) as (58 mm, 35 mm, 4 mm), (60 mm, 37 mm, 6 mm) and (60 mm, 38 mm, 8 mm) respectively (the pinna size of the 12 year old child MRI-based model is 59 mm, 33 mm and 10 mm). To take into account the influence of the shape of the head, three other head models have been created (see figure 5). Using the shape distribution of the 12 years old age class (Farkas 1994) two models have been created with parameters (height, width, etc.) set up to their means ± 2 standard deviations. The third model corresponds to the mean value of the 12 years old age class. To take into account a phone on the left or right position two other models have been built. Overall eight configurations representing various possibilities have been built.

3. Handset models

Sources modeling must be handled with care since a dipole, a monopole on a box or a handset having a patch antenna have not the same radiation pattern and will not induce the same SAR distribution in the tissues. The sources used as a handset in this study are a dipole (named here after dipole mobile phone (DMP)), a generic mobile phone (GMP) and a commercial mobile phone (CMP) shown in figure 6. The GMP, described in previous studies (Kainz *et al* 2005, Beard *et al* 2006), looks like a handset having a monopole antenna on a metal box covered by plastic.

The CMP described in the literature (Hadjem *et al* 2005) is a realistic model since it is composed of a plastic box, a display, a keyboard and an inside battery, a printed circuit board and a patch antenna (figure 6). This model is of interest since it allows a realistic positioning and complex devices to estimate a realistic SAR. In all the cases, the sources are located near the head in a 'cheek position' which is representative and well defined in the standards such as CENELEC EN 50361 or IEC 62209-1.

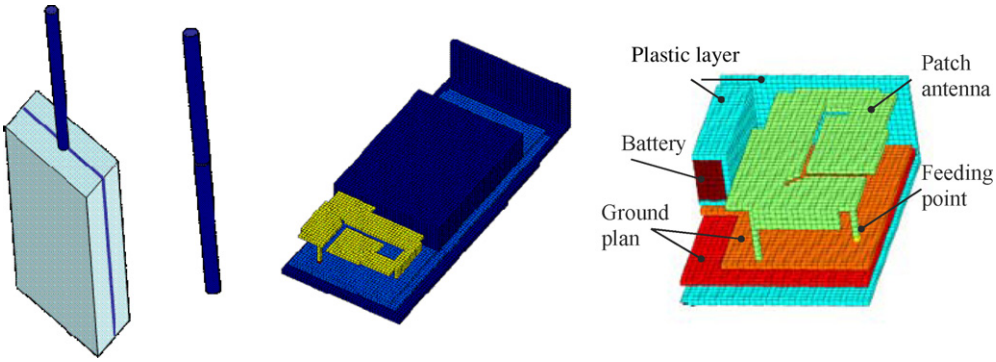

Figure 6. Sources representing a handset used in this study (from left to right): GMP, DMP, CMP and internal view of the CMP.

The maximum power emitted by a handset depends on the frequency band and on the multiple access technique. It also depends on the design itself (antenna location, antenna mismatch, internal load, etc.). Because of that, in this paper, since the objective is not to check the compliance of a given handset, we assume a perfect matching, no loss with a power emitted set up to have the maximum SAR over 10 g in VH equal to 1 W kg^{-1}. As a consequence, the possible influences of the variation of body tissues on mismatching and therefore on induced SAR are neglected and we focus on the influence of the morphology.

4. SAR estimation in the head models

The SAR is given by the well-known relationship

$$\mathrm{SAR} = \frac{\sigma E^2}{\rho}. \tag{1}$$

In equation (1), σ represents the conductivity, E the rms (root mean squares) electric field strength in tissues and ρ the mass density. Different numerical methods can be used to estimate the SAR. The well-known method FDTD (finite difference in time domain) that has been intensively studied (Yee 1966, Taflove and Hagness 2000) has been used in the present study by means of an in-house FDTD code with perfectly-matched layers (Berenger 1994) as absorbing boundary conditions. The code has been validated with canonical cases (Conil *et al* 2008) and has been used in other studies (Beard *et al* 2006).

In both ICES (IEEE 2005) and ICNIRP (ICNIRP 1998), local SAR is estimated as an average over 10 g of tissues, but ICNIRP recommends use of continuous tissues while ICES use of a tissue volume with the shape of a cube. To check the compliance of equipment, IEC (IEC 62209-1) also used a volume in the shape of a cube to estimate the maximum SAR over 10 g (MSAR10g). Thus, most SAR studies are performed over a cube (Christ and Kuster 2005, Beard *et al* 2006). To allow comparisons with previous studies, we decided to assess the MSAR10g using a cube shape.

To analyze the exposure of particular tissues, 10 g could be quite large since with a skin having a thickness of 2 mm this leads to the involvement of a surface larger than 7 cm $\times$ 7 cm. On the other hand, due to stair case problem, the accuracy of the FDTD is limited locally. Therefore, we preferred the averaging of the SAR over a smaller volume of 1 g. To estimate the maximum SAR over such 1 g (MSAR1g) of a given tissue the cube shape is not relevant

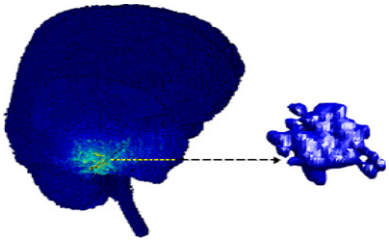

Figure 7. SAR distribution in the brain (left) of a 15 year old child and the shape of the 1 g volume having maximum SAR (source: CMP operating at 1800 MHz).

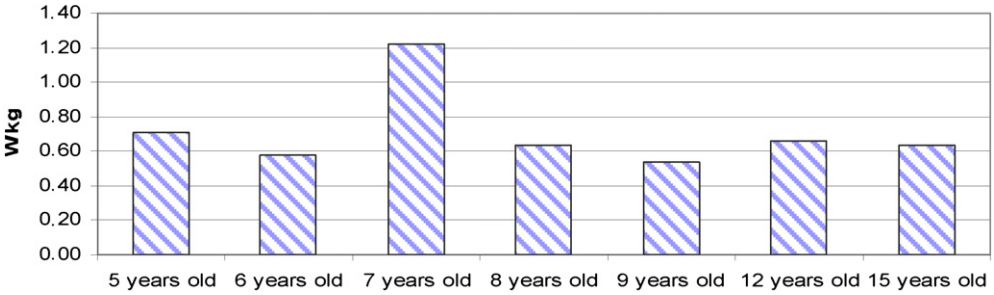

Figure 8. MSAR10g induced by CMP operating at 900 MHz in the different child head models (power emitted by the handset corresponding to an MSAR10g of 1 W kg^{-1} in VH).

since such a cube often covers many different tissues. Thus in this study the MSAR1g in a given tissue is estimated by the summation of the highest SAR in voxels of this tissue up to having one gram. Since the volume is quite small and the exposure is localized, the volume is composed of continuous tissues. In the case of brain, the volume of 1 g in which the SAR is maximum can have different shapes. Figure 7 shows such a shape with a handset operating at 1800 MHz and the brain of a 15 year old child.

5. Comparisons and discussions

5.1. Maximum SAR over 10 g

The MSAR10g has been estimated in the different head models with the different sources and frequencies as explained previously. Figure 8 shows the MSAR10g in child head models exposed to a handset operating at 900 MHz. The SAR values are normalized to the emitted power giving an MSAR10g of 1 W kg^{-1} in VH. As can be seen, the variability is important, which confirms the influence of shape and anatomy of the heads. For instance, dealing with the CMP operating at 900 MHz, the MSAR10g in child head models (normalized such that the MSAR10g in VH is 1 W kg^{-1}) varies from 0.53 W kg^{-1} to 1.22 W kg^{-1}. The mean value of the MSAR10g is equal to 0.71 W kg^{-1} with a standard deviation of 0.23 W kg^{-1} (32% of the mean value). With the same source (CMP) operating under the same condition the MSAR10g in adult head models (still normalized such that the MSAR10g in VH is 1 W kg^{-1}) varies between 0.3 W kg^{-1} and 1 W kg^{-1} (mean 0.56 W kg^{-1}, standard deviation 0.24 W kg^{-1} or 42% of the mean value). It has to be noted that since we have no information

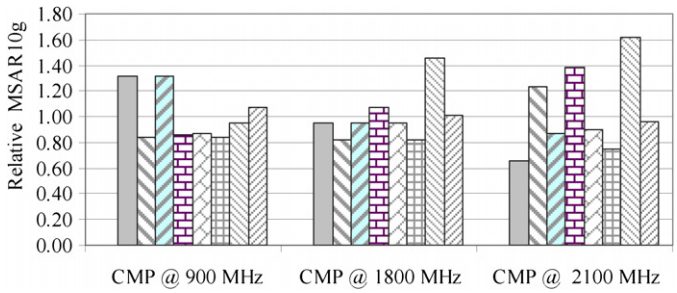

Figure 9. Relative MSAR10g induced by CMP in the different 12 year old child head models (MSAR10g normalized to the mean value in each band).

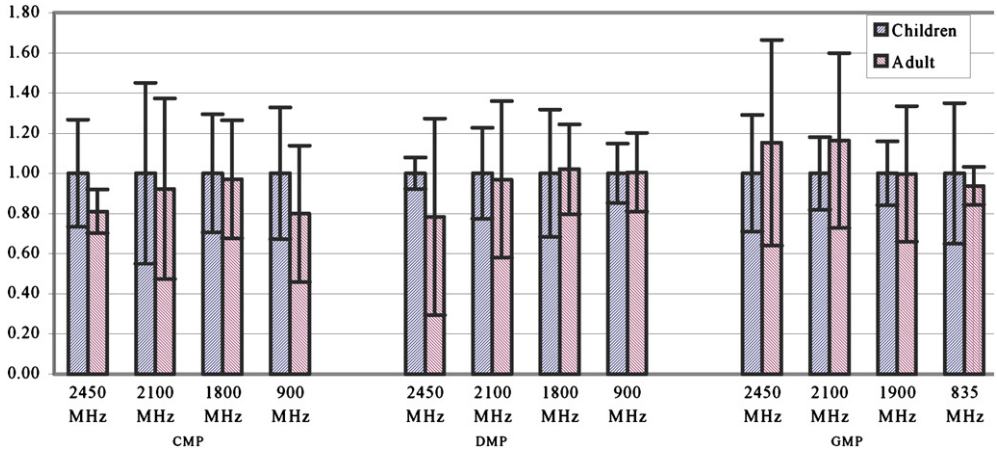

Figure 10. Relative mean MSAR10g in child and adult MRI-based head models (mean MSAR10g normalized to mean MSAR10g in child head models) with their standard deviations.

on the statistical law, the standard deviation cannot be linked to any quintiles, nevertheless it provides information on the average spreading of the data.

Since the child heads of a same age class are varying, we analyze the variation of the MSAR10g in the 12 years old age class. Using morphing techniques, eight different child head models have been built and simulations performed with the model of a commercial phone. In this case the MSAR10g has been normalized to the mean value obtained in each band.

Figure 9 shows the MSAR10g obtained with this normalization at the frequencies of 900 MHz, 1800 MHz and 2100 MHz. As can be seen, the variations are large and comparable to those observed in a previous study (Christ and Kuster 2005). The standard deviations are 20% at 900 MHz and 1800 MHz while the standard deviation is 33% at 2100 MHz. With all the data the standard deviation is 24%. The same processing has been done with the same handset and the adult head models; in this case the standard deviation is 30%.

The maximum SAR over 10 g has been estimated in adult and child MRI-based head models with different RF sources (DMP, GMP, CMP) operating at different frequencies. Mean values and standard deviations have been calculated. Figure 10 summarizes the results. The differences between the mean values are small compared to the standard deviations. The standard deviations are quite important (the ‘mean’ standard deviation is about 30% of the

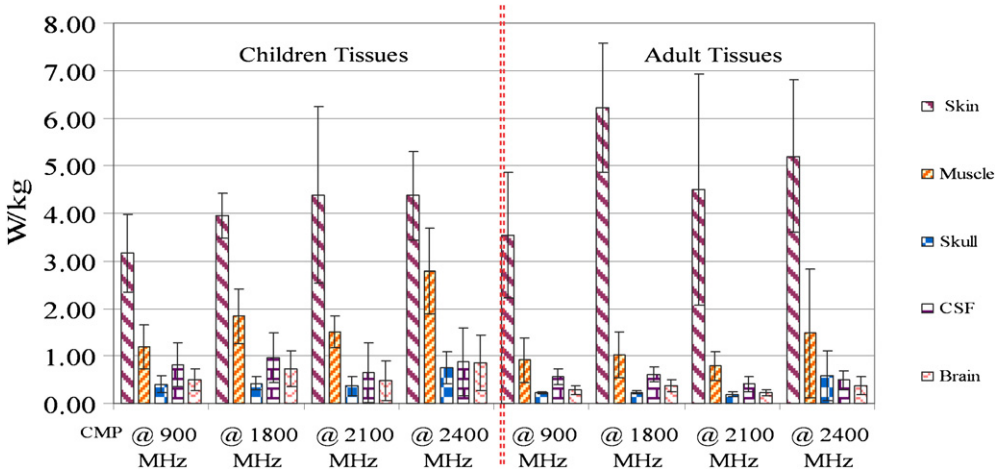

Figure 11. Mean MSAR 1g of tissues induced by the CMP in child and adult head models tissues (input power set up to induce an MSAR10g of 1 W kg^{-1} in VH).

mean value but in some cases the standard deviation can be larger). Considering the simulations that have been performed the maximum SAR over 10 g in adults and those induced in child head models are similar. These results support the conclusion of previous studies (Beard *et al* 2005, Christ and Kuster 2005).

5.2. Brain exposure

The MSAR10g is important, nevertheless it is also of interest to analyze the exposure of specific tissues. Therefore, the MSAR1g in each tissue has also been studied with an emitted power set up at a level inducing an MSAR10g of 1 W kg^{-1} in VH. Figure 11 shows the MSAR1g induced by the CMP operating at various frequencies in the tissues of child and adult MRI-based head models.

The brain and the cerebellum exposure are of particular interest for biomedical study. A previous study (Kuster *et al* 2004) has been carried out but while several handsets were involved only one head model has been used. Moreover the exposure was estimated at a given point and not at the maximum. In the present study we analyzed at different frequencies and using different sources the ratio of the MSAR1g in cerebellum to the MSAR1g in brain of adult head models. In cheek position and for all the frequency and sources the mean value of such a ratio is 0.47 with a standard deviation of 0.07. The result obtained in this study must be handled carefully since only the cheek position has been investigated and since such a ratio can be influenced by the position of the phone. Nevertheless it is of interest to point out that the frequency band does not influence significantly the ratio, for instance the ratio estimated with the commercial phone is 0.43 at 900 MHz, 0.32 at 1800 MHz, 0.46 at 2100 MHZ and 0.38 at 2400 MHz. This is probably due to the fact that the higher exposed areas in the brain and in the cerebellum are close to each other (figure 12).

The brain of children is from the volume point of view quite similar to the adult brain (Huttenlocher 1979, Reissenweber *et al* 2005). Nevertheless the surrounding tissues are different, it is then important to analyze the spatial distribution of the SAR. In a previous study (Kainz *et al* 2005) the max SAR over 1 g of tissues (and not a specific tissue such as

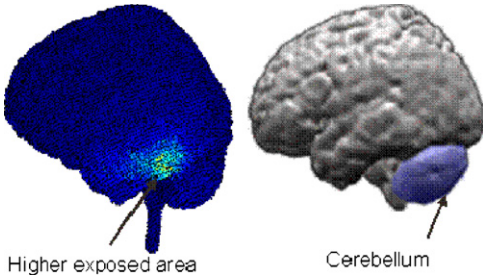

Figure 12. Localization of the higher exposed area of the brain and the cerebellum.

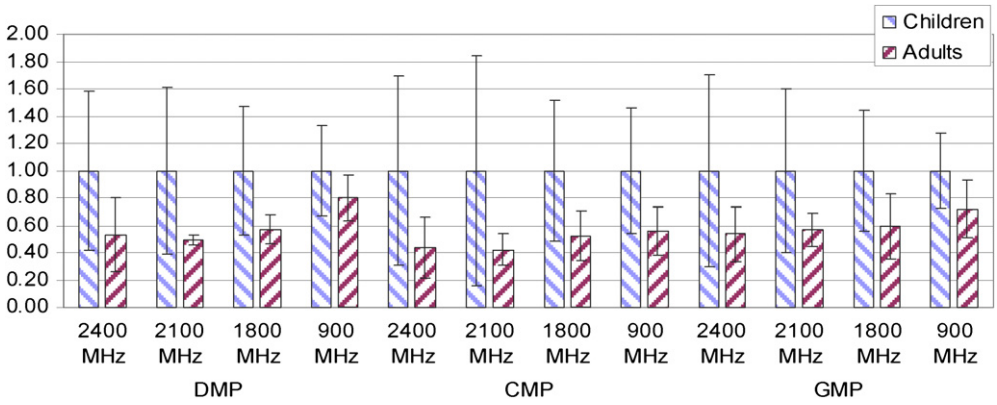

Figure 13. Relative mean MSAR1g of adult and child brain tissues (normalized to children).

brain) was estimated numerically in 14 different anatomical models of adults, scaled adults and children. The results of this study show large differences in the maximum SAR over 1 g but not correlated to the age but this study did not analyze the brain exposure. In the present study we investigate specifically the MSAR1g in brain through the analysis of the ratio of MSAR1g estimated in adult and child brain tissues. Figure 13 shows the results and indicates a large variability of such ratio that depends not only on the frequency but also on the shape of the handset.

This analysis confirms that the peripheral brain tissues of children seem to be higher exposed than the peripheral brain tissues of adults. Definitive conclusion must take into account the large variability of the data. Nevertheless such results are not unexpected since the smaller thicknesses of the pinna, skin and skull of children (compared to adult ones) leads to a reduced distance from the handset to the peripheral brain tissues inducing by the way a higher exposure.

Since the standard deviation is quite important in the children data and since the thicknesses of skin, pinna and skull depend on the age, we analyze the previous ratios in sub-populations of children. The total population has been split into two groups (above 8 years old and strictly below 8 years old). Figure 14 shows for brain tissues the ratio of the MSAR1g obtained in children younger than 8 years old and older than 8 years old.

The ratio between MSAR1g in brain tissues of children (8–15 years old) and MSAR1g in brain tissues of children (5–8 years old) varies from 0.3 to 0.7 with a mean and median equal

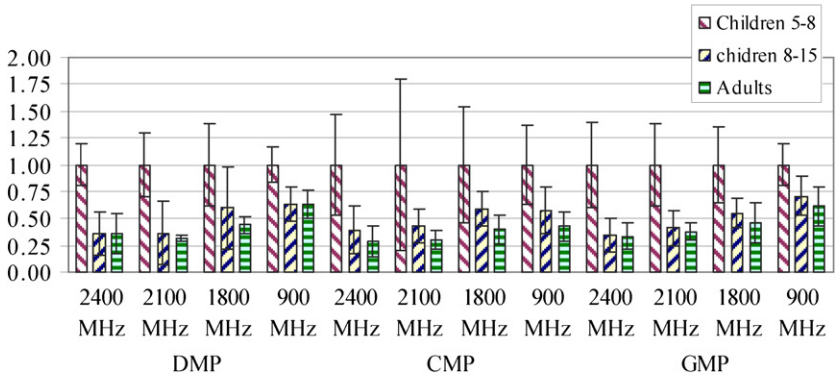

Figure 14. Relative mean MSAR1g in brain tissues of children and adults.

to 0.5 and a standard deviation of 0.1. The same analysis has been done between adults and children (5–8 years old). In this case the ratio varies from 0.3 to 0.6 with a mean and a median equal to 0.4.

The MSAR1g in brain tissues of (8–15 years old) is comparable to the one of adults while the MSAR1g in brain of (5–8 years old) is higher than the one of adults. As has been pointed out in the previous sections, the SAR depends on the tissues properties, on the morphology and on the position of the mobile phone that can change with age. Thus, the SAR induced by a same source in different heads is highly varying. The large variability of human morphology, the limited number of phantoms and the influence of voxel size on tissues thicknesses may enlarge the spreading of the results and influence the results obtained in the present study.

6. Conclusions

The analysis of RF exposure in child and adult heads has often been performed in a very limited number of models. Since there is a large variability of human morphology, comparisons between adults and children as well as the SAR distribution in brain must be carried out with several child and adult head models. In this study several child head models have been developed to cover ages ranging from 5 to 15 years old to be compared to six adult head models developed in different international laboratories. The anatomy of the models used has been analyzed and compared. Simulations have been performed with the well-known FDTD and by using three sources (a dipole, a commercial handset having a patch antenna and a generic handset having a quarter wavelength antenna) operating in cheek position at 900, 1800, 2100 and 2400 MHz.

Considering the simulations that have been performed the maximum SAR over 10 g estimated in the head models of the adults and children are about the same since the differences are small compared to the standard deviations. The comparisons have also shown that the maximum SAR in 1 g of peripheral brain tissues of child models aged between 8 and 15 is comparable to the maximum SAR in 1 g of peripheral brain tissues of adult models while it is about two times higher for child models aged between 5 and 8. This is certainly due to the smaller thicknesses of pinna, skin and skull.

The present study points out the influence of the variability of the human morphology. The SAR induced by a same source in different head models is varying with a standard deviation of 30% for maximum SAR over 10 g and about 50% for the maximum SAR over 1 g in the

brain. The results obtained in this study need to be confirmed since they have been derived from data sets of limited size. Nevertheless these results are comparable to those obtained in other studies involving several phantoms (Beard *et al* 2006, Kainz *et al* 2005).

Since many years, major efforts have been carried out to improve the numerical dosimetry and numerical methods and in particular the FDTD has been improved and adapted to this domain. The question of assessing and managing the uncertainty is now the main challenge of the dosimetry.

Acknowledgments

The authors would like to thank S Watanabe from the National Institute of Information and Communication Technology (NICT), Japan, A K Lee from the Electronics and Telecommunications Research Institute (ETRI) Korea, P Dimbylow from the Health Protection Agency (HPA), UK, and P Mason and J Ziriax from Brooks Air Force, USA, for providing head models. The authors would also like to thank the French hospitals of Nîmes, Paris Necker and Paris Saint Vincent de Paul which provided the MRI data of child heads. This study has been funded by the French Research Agency (ANR–RNRT Program ADONIS project).

References

Beard B *et al* 2006 Comparisons of computed mobile phone induced SAR in the SAM phantom to that in anatomically correct models of the human head *IEEE Trans. EMC* **48** 397–407

Berenger J P 1994 A perfectly matched layer for the absorption of electromagnetic waves *J. Comput. Phys.* **4** 185–200

Burguet J, Gadi N and Bloch I 2004 Realistic models of children heads from 3D MRI segmentation and tetrahedral mesh construction *2nd Int. Symp. on 3D Data Processing, Visualization and Transmission, 3DPTV (Thessaloniki, Greece)* pp 631–8

CENELEC 2001 Norme Européenne basic standard for the measurement of specific absorption rate related to human exposure to electromagnetic fields from mobile phones (300 MHz–3 GHz) CENELEC EN 50361 http://www.cenelec.eu

Christ A and Kuster N 2005 Differences in RF energy absorption in the heads of adults and children *Bioelectromagnetics* **26** (Suppl. 7) S31–44

Collatz-Christensen H, Schüz J, Kosteljanetz M, Skovgaard Poulsen H, Boice J D, McLaughlin J K and Johansen C 2005 Cellular telephones and risk for brain tumors. A population-based, incident case-control study *Neurology* **64** 1189–95

Conil E, Hadjem A, Lacroux F, Wong M F and Wiart J 2008 Variability analysis of SAR from 20 MHz to 2.4 GHz for different adult and child models using FDTD *Phys. Med. Biol.* **53** 1511–25

Dasembrock C 2005 Animal carcinogenicity studies on radiofrequency fields related to mobile phones and base stations *Toxicol. Appl. Pharmacol.* **207** S342–6

De Salles A A, Bulla G and Rodriguez C E 2006 Electromagnetic absorption in the head of adults and children due to mobile phone operation close to the head *Electromag. Biol. Med.* **25** 349–60

Dimbylow P J 1997 FDTD calculations of the whole-body averaged SAR in an anatomically realistic voxel model of the human body from 1 MHz to 1 GHz *Phys. Med. Biol.* **42** 479–90

Dokladal P, Bloch I, Couprie M, Ruijters D, Urtasun R and Garnero L 2003 Topologically controlled segmentation of 3D magnetic resonance images of the head by using morphological operators *Pattern Recognit.* **36** 2463–78

Drossos A, Santomaa V and Kuster N 2000 The dependence of electromagnetic energy absorption upon human head tissue composition in the frequency range of 300–3000 MHz *IEEE Trans. Microw. Theory Tech.* **48** 1988–95

EMF Project 1996 http://www.who.int/peh-emf/project/en/

Farkas L G 1994 *Antropometry of the Head and Face* (New York: Raven Press)

Gabriel C 1996 Compilation of the dielectric properties of body tissues at RF and microwave frequencies *Brooks Air Force Technical Report* AL/OE-TR-1996-0037

Gandhi O P, Lazzi G and Furse C 1996 Electromagnetic absorption in the human head and neck for mobile telephones at 835 MHz and 1900 MHz *IEEE Trans. Microw. Theory Tech.* **44** 1884–97

Hadjem A, Lautru D, Dale C, Man Fai Wong, Hanna V F and Wiart J 2005 Study of specific absorption rate (SAR) induced in the two child head models and adult heads using a mobile phones *IEEE Trans. Microw. Theory Tech.* **53** 4–11

Huttenlocher P R 1979 Synaptic density in human frontal cortex—developmental changes and effects of aging *Brain Res* **163** 195–205

ICNIRP 1998 Guidelines for limiting exposure to time varying electric magnetic and electromagnetic field (up to 300 GHz) *Radiat. Prot. Health Phys.* **74** 494–522

IEC 2005 Human exposure to radio frequency fields from hand-held and body-mounted wireless communication devices—Human models, instrumentation, and procedures: Part 1. Procedure to determine the specific absorption rate (SAR) for hand-held devices used in close proximity to the ear (frequency range of 300 MHz to 3 GHz) *Standard Int. Electrotechnical Commission (IEC)* Std 62209-1

IEEE 2005 Standard for safety levels with respect to human exposure to radio frequency electromagnetic fields, 3 kHz to 300 GHz Std C95.1 http://www.ieee.org

Juutilainen J 2005 Developmental effects of electromagnetic fields *Biolectromagnetics* **S7** 107–15

Kainz W, Christ A, Kellom T, Seidman S, Nikoloski N, Beard B and Kuster N 2005 Dosimetric comparison of the specific anthropomorphic mannequin (SAM) to 14 anatomical head models using a novel definition for the mobile phone positioning *Phys. Med. Biol.* **50** 3423–45

Keshvari J, Keshvari R and Lang S 2006 The effect of increase in dielectric values on specific absorption rate (SAR) in eye and head tissues following 900, 1800 and 2450 MHz radio frequency (RF) exposure *Phys. Med. Biol.* **51** 1463–77

Kheifets L, Repacholi M, Saunders R and Van Deventer E 2005 The sensitivity of children to electromagnetic fields *Pediatrics* **116** 303–13

Kim J I, Choi H, Lee B I, Lim Y K, Kim C S, Lee J K and Lee C 2006 Physical phantom of typical Korean male for radiation protection purpose *Radiat. Prot. Dosim.* **118** 131–6

Kuster N, Schuderer J, Christ A, Futter P and Ebert S 2004 Guidance for exposure design of human studies addressing health risk evaluations of mobile phones *Bioelectromagnetics* **25** 524–9

Lee A K, Choi H D and Choi J I 2007 Study on SARs in head models with different shapes by age using SAM model for mobile phone exposure at 835 MHz *IEEE Trans. EMC* **49** 302–12

Lichtenecker L 1926 Die dielektrizitatskonstante naturlicher und kunstlicher mischkorper *Physikalische Zeitschrift* **27** 115–8

Martens L 2005 Electromagnetic safety of children using wireless phones: a literature review *Bioelectromagnetics* **26** (Suppl. 7) S133–7

Mochizuki S, Wakayanagi H, Hamada T, Watanabe S, Taki M, Yamanaka Y and Shirai H 2007 Effects of ear shape and head size on simulated head exposure to a cellular phone *IEEE Trans. EMC* **49** 512–8

MTHR (Mobile Telephony Health Research Program) 2007 *Report* www.mthr.org.uk/documents/MTHR_report_2007.pdf

Nagaoka T, Watanabe S, Sakurai K, Kunieda E, Taki M and Yamanaka Y 2004 Development of realistic high-resolution whole-body voxel models of Japanese adult males and females of average height and weight, and application of models to radio-frequency electromagnetic-field dosimetry *Phys. Med. Biol.* **49** 1–15

Peyman A, Razazadeh A A and Gabriel C 2002 Change in the dielectric properties of rat tissue as a function of age at microwave frequencies *Phys. Med. Biol* **47** 2187–8

Reißenweber J, Poess Janine and David Eduard 2005 Sensitivity of children to EMF exposure—do elevated susceptibilities to high-frequency mobile communication fields exist during discrete developmental phases? Edition *Wissenschaft* FGF Funk e V G 14515 (22)

Repacholi M, Saunders R, Van Deventer E and Kheifet L 2005 Guest editors' introduction: is EMF a potential environmental risk for children? *Bioelectromagnetics* **26** S2–4

Schoenborn F, Burhardt V and Kuster N 1998 Difference in energy absorption between heads of adults and children in the near field of sources *Health Phys.* **74** 160–8

Seidenari S *et al* 2000 Thickness and echogenicity of the skin in children as assessed by 20 MHz ultrasound *Dermatology* **201** 218–22

Serra J 1982 *Image Analysis and Mathematical Morphology* (New York: Academic)

SSI 2006 Recent Research on EMF and Health Risks Fourth annual report from SSI's Independent Expert Group on Electromagnetic Fields (www.ssi.se/ssi_rapporter/pdf/ssi_rapp_2007_4.pdf)

Taflove A and Hagness S 2000 *Computational Electrodynamics* (Boston, MA: Artech House)

Tillmann T, Ernst H, Ebert S, Kuster N, Behnke W, Rittinghausen S and Dasenbrock C 2007 Carcinogenicity study of GSM and DCS wireless communication signals in B6C3F1 mice *Bioelectromagnetics* **28** 173–87

Visible Human Project National Library of Medicine www.nlm.nih.gov/research/visible

Wang J and Fujiwara O 2003 Comparison and evaluation of electromagnetic absorption characteristics in realistic children for 900-MHz mobile telephones *IEEE Trans. Microw. Theory Tech.* **51** 966–71

Wang J, Fujiwara O and Watanabe S 2006 Approximation of aging effect on dielectric tissue properties for SAR assessment of mobile telephones *IEEE Trans. EMC* **48** 408–13

Watanabe S, Taki M, Nojima T and Fujiwara O 1996 Characteristics of the SAR distributions in a head exposed to electromagnetic fields radiated by a hand-held portable radio *IEEE Trans. MTT* **44** 1874–83

Wiart J, Hadjem A, Gadi N, Bloch I, Wong M F, Pradier A, Lautru D, Hanna V F and Dale C 2005 Modeling of RF exposure in children *Bioelectromagnetics* **26** 45–50

Xu C and Prince J Snakes 1998 Shapes, and gradient vector flow *IEEE Trans. Image Process.* **7** 359–69

Yee K S 1966 Numerical solution of initial boundary value problems involving Maxwell's equations in isotropic media *IEEE Trans. Antennas Propagat* **14** 302–7

Zubal I G, Harrell C R, Smith E O, Rattner Z, Gindi G and Hoffer B P 1994 Computerized 3-dimensional segmented human anatomy *Med. Phys.* **21** 299–302